Development and characterization of a humanized mouse model of osteoarthritis

B. Bodic, M.A. Boutet, C. Boyer, B. Metayer, C. Vignes, J. Lesoeur, J. Veziers, V. Daguin, F. Haspot, Y. Maugars, et al.

DEVELOPMENT AND CHARACTERIZATION OF A HUMANIZED MOUSE MODEL OF OSTEOARTHRITIS

Bodic B.[1,2], Boutet M.A.[1,2,3], Boyer C.[1,2], Metayer B.[1,4], Vignes C.[1,2,5], Lesoeur J.[1,2,5], Veziers J.[1,2,5,6], Daguin V.[7], Haspot F.[7], Maugars Y.[1,4], Djouad F.[8]*, Guicheux J.[1,2,6]*, and Vinatier C.[1,2,]*

[1] Inserm, UMR 1229, Regenerative Medicine and Skeleton, University of Nantes, ONIRIS, Nantes, France

[2] University of Nantes, UFR Odontologie, Nantes, F-44042, France

[3] Centre for Experimental Medicine & Rheumatology, William Harvey Research Institute and Barts and The London School of Medicine and Dentistry, Queen Mary University of London; London, UK.

[4] CHU Nantes, Service rhumatologie, PHU4 OTONN, Nantes, F-44093, France

[5] INSERM, UMS 016, CNRS 3556, Structure Fédérative de Recherche François Bonamy, SC3M facility, CHU Nantes, University of Nantes, Nantes, F-44042 France

[6] CHU Nantes, PHU4 OTONN, Nantes, F-44093, France

[7] Inserm, Université de Nantes, Centre de Recherche en Transplantation et Immunologie, UMR 1064, ITUN, F-44000 Nantes, France

[8] IRMB, Univ Montpellier, INSERM, Montpellier, France

* These authors contributed equally to this work

Co-corresponding authors: Jerome Guicheux & Claire Vinatier

Address: INSERM, UMR 1229, Regenerative Medicine and Skeleton, University of Nantes, ONIRIS, Nantes, France

E-mail: jerome.guicheux@univ-nantes.fr; claire.vinatier@univ-nantes.fr

Tel: +33 2 40 41 29 19

ABSTRACT

Objective: In light of the role of immune cells in OA pathogenesis, the development of sophisticated animal models closely mimicking the immune dysregulation during the disease development and progression could be instrumental for the preclinical evaluation of novel treatments. Among these models, immunologically humanized mice may represent a relevant system, particularly for testing immune-interacting DMOADs or cell therapies before their transfer to the clinic. Our objective, therefore, was to develop an experimental model of OA by destabilization of the medial meniscus (DMM) in humanized mice.

Method: Irradiated 5-week-old NOD/LtSz-scid IL2Rγ^{null} (NSG) mice were humanized by intravenous injection of $CD34^+$ human hematopoietic stem cells. The engraftment efficiency was evaluated by flow cytometry 17 weeks after the humanization procedure. Humanized and non-humanized NSG mice underwent DMM or sham surgery and OA development was assessed 1, 6, and 12 weeks after the surgery.

Results: 120 days after the humanization, human T and B lymphocytes, macrophages and NK cells, were present in the blood and spleen of the humanized NSG mice. The DMM surgery induced articular cartilage and meniscal alterations associated with an increase in OA and the meniscal score. Moreover, the surgery triggered an inflammatory response that was sustained at a low grade in the DMM group.

Conclusions: Our study shows for the first time the feasibility of inducing OA by DMM in humanized mice. This novel OA model could constitute a useful tool to bridge the gap between the preclinical and clinical evaluation of immune interacting DMOADs and cell-based therapies.

Keywords

Osteoarthritis, animal model, humanized mouse, DMM

55 *Running Title*

56 Humanized mouse model of osteoarthritis

INTRODUCTION

Osteoarthritis (OA) is the most common inflammatory and degenerative joint disease in humans. Chronic low-grade inflammation in OA, characterized by synovitis and a pro-inflammatory/catabolic state of the chondrocytes in the majority of patients[1], involves both the innate and adaptive immune systems and is actively involved in the disease progression[2-4]. The inflammatory process in OA is triggered in particular by cartilage or meniscal degradation products, called damage-associated molecular patterns (DAMPS), that activate various cell types in the joint (macrophages, fibroblasts, and chondrocytes). Activated cells in the synovial membrane and cartilage respond by the production of chemoattractants, inflammatory cytokines (interleukins (IL-6, IL-1β) and tumor necrosis factor-alpha (TNF-α)), growth factors (transforming growth factor–β (TGFβ) and insulin-like growth factor-1 (IGF-1)), and matrix-degrading enzymes (matrix metalloproteases (MMPs) such as a disintegrin and metalloprotease with thrombospondin motifs (ADAMTS), etc.), thereby leading to synovial immune cell (monocytes/macrophages) infiltration, cartilage degradation, and osteophyte development[1]. Given the pathogenic role of low-grade inflammation, disease-modifying osteoarthritis drugs (DMOADs) that target inflammatory cytokines, such as anti-IL-1β, anti-IL-6, and anti-TNF-α, have been developed. However, although these entities have yielded promising results in preclinical studies, notably in murine models of OA, they have so far failed to exhibit a significant degree of clinical efficacy in humans[5]. This low level of clinical predictivity of murine OA models[6] may at least in part be explained by the numerous differences in the immune system and inflammatory processes between humans and mice[7]. These differences affect both innate and adaptive immunity and they include the balance of leukocyte subsets, NK inhibitory receptor families, B and T cell signaling pathways, Th1/Th2 differentiation, and the expression and function of costimulatory molecules[8,9]. This discrepancy between mice and humans is also observed in response to

inflammatory stress at the genomic level[7]. More particularly, species-specific differences in TLR expression and macrophages metabolism[9]are relevant in the OA context.

To overcome the poor level of human clinical predictability of mouse models, notably for inflammation- and immune-related diseases, humanized mice have been considered. The generation of humanized mice was enabled by several major improvements in the generation of immunodeficient mice. The third generation of immunodeficient mice, the NOD.Cg-*Prkdc*^{scid} *Il2rg*^{tm1Wjl} (NSG) mice, combine the SCID (*Prkdc*^{Scid}) mutation in the NOD background and mutation of the interleukin-2 receptor (IL-2R) γ-chain locus (*IL2rγ* gene). These NSG mice exhibit total impairments in NK-cell, T-cell, and B-cell development as well as hypofunction of innate immune cells such as monocytes/macrophages, dendritic cells, and neutrophils[10,11] associated with an increased lifespan. These mice support long-term engraftment of human hematopoietic stem cells (HSC) that can undergo multilineage development over time, resulting in a poly-functional human immune system, including T, B, NK, and dendritic cells, as well as monocytes/macrophages and granulocytes[12]. These humanized mouse models have been widely used in various research areas such as oncology[13], transplantation[14], and autoimmunity[15].

Whereas humanized mice have been generated to investigate the mechanisms governing acute inflammatory rheumatoid arthritis, including the migration of human immune cells into the joint and the pathogenic role of TNF-α[16], to our knowledge, a model of OA humanized mice has not yet been described. In light of this and the role of immune cells and low-grade inflammation in the pathogenesis of OA, our objective was to develop an experimental model of OA in humanized mice. After having validated the humanization of these mice, post-traumatic OA was surgically induced by destabilization of the medial meniscus, and the OA features were investigated.

MATERIALS AND METHODS

Mice

The NOD.Cg-Prkdc^{scid} Il2rγ^{tm1Wjl} immunodeficient mice (NSG, stock #05557, the Jackson Laboratory (Bar Harbor, ME, USA) were bred at the Humanized Rodent Platform of LabEx IGO and were housed in the Nantes University UTE IRS-UN animal facility under specific pathogen-free conditions according to institutional guidelines (accreditation number C44-278). This study was performed according to the European guidelines for the care and use of laboratory animals (2010/63/EU) and authorization from the French Ministry of Research (APAFIS #7437-2016110213027604).

Humanization procedure

Five-week-old NSG female mice were irradiated sublethally (1.5 Gy) and infused intravenously with 50 x 10^3 human CD34$^+$ mononuclear cells (Lonza, NJ, USA) 3 days later. To validate the humanization, peripheral blood was harvested and the immune cell subpopulations were assessed using the antibodies listed in table 1. Flow cytometric analyses were performed on a BD FACSCanto II™ Cell Analyzer (BD Biosciences, CA, USA). The humanized mice (n=37) were included in the OA induction protocol after achieving sufficient immune blood reconstitution (i.e. engraftment efficiency (%graft) > 10%) (Fig 1 A, B).

DMM procedure

Post-traumatic osteoarthritis was experimentally induced in non-humanized and humanized mice by unilateral (right knee) destabilization of the medial meniscus (DMM) 17 weeks post-humanization. At 22 weeks-old, non-humanized and humanized mice were randomly taken from their cage for OA induction by DMM (non-humanized n=9; humanized n=21). The DMM surgery was performed on anesthetized mice according to the procedure of Glasson *et al.*[17]. A second group of mice (non-humanized n=7; humanized n=16) underwent a sham

procedure. The non-humanized and humanized mice were sacrificed 6 and 12, and 1, 6, and 12 weeks after the surgery respectively. Blood samples of humanized mice were harvested 6 and 12 weeks after the surgery. At each time point, spleen (only for humanized mice) and knee joints were also harvested and fixed in a 4% w/v paraformaldehyde for 48 h.

Microtomography

The knee joints were analyzed with µCT according to Bouxsein *et al.*'s guidelines[18] using a micro-computed tomography Skyscan 1272® device (Bruker, Germany) with a 5-µm isotropic voxel size (50 kV, 200 µA, 0.45° rotation angle). 3D reconstructions were performed using NRecon software (Bruker) followed by spatial orientation using Dataviewer® software (Bruker). To assess subchondral bone changes, CT-Analyser® software (Bruker) was used to define a 160µm diameter cylindrical regions of interest (ROI) from the bone surface to the growth plate in the medial tibial epiphysis, this ROI was further divided into a cortical and a trabecular area (Supplementary Fig. 1A). The medial meniscus (including anterior and posterior areas) was also selected for analysis. Structural bone parameters, including bone volume (BV; mm^3) and trabecular thickness (Tb.Th; mm) were quantified using 3D algorithms in CT-Analyser® software (Bruker). 3D models of the tibia menisci were created using CTVox software (Bruker).

Histology and scoring

The knee joints were decalcified using TBD-2 solution (Thermo Scientific, MA, USA) for 48 h at 4 C before being embedded in paraffin (Leica TP1020 automated tissue processor, Germany). Serial 5-µm thick coronal sections were made using a 2050 Supercut microtome (Leica Microsystems). Safranin-O fast green staining was carried out using standard histological procedures.

The OA severity was evaluated using a modified Osteoarthritis Research Society International (OARSI) scoring system (Table 2) as previously described[19-21]. The OA scores were

expressed as the mean of the four quadrants. Meniscal damage was scored according to criteria devised by Kwok *et al.*[3]. Synovial inflammation was assessed by a synovitis score developed by Lewis *et al.*[22]. Scoring was performed blindly and independently by three different readers (BB, JL, and CV) on at least three levels of the joint for each sample.

Immunohistochemistry and image analysis

Immunohistochemistry was performed on deparaffinized and rehydrated sections with specific primary antibodies listed in table 1. The primary antibodies were detected using a kit (DAKO, Agilent, CA USA) with DAB substrate, and the sections were counterstained using Mayer's hematoxylin (RAL Diagnostic, Martillac, France). As a negative control, sections were processed with identical protocols but without the primary antibody. Tissue samples harvested from non-humanized NSG mice were used as negative controls for the detection of human cells. The histological sections were finally observed using a NanoZoomer 2.0 Hamamatsu slide scanner (Hamamatsu Photonics, Hamamatsu, Japan).

Statistical analysis

GraphPad Prism 8.0v software (GraphPad, CA, USA) was used for the statistical analyses. We have used nonparametric tests. The Mann-Whitney test was used for comparison of only two groups. To compare three or four conditions, we used the Kruskal-Wallis test followed by Dunn's multiple comparison test. A p-value of less than 0.05 was considered to be statistically significant.

RESULTS

An overview of the experimental procedure used for this study is presented in Figure 1A. After the humanization procedure on day 0 (D0) by intravenous (IV) injection of human HSCs, the mice underwent a DMM or sham surgical procedure 17 weeks post-humanization.

The mice were ultimately sacrificed at 1, 6, and 12 weeks after OA induction for all of the subsequent analyses.

Generation and characterization of the humanized mice

To validate the humanization procedure, the engraftment efficiency was determined for each mouse. Our data (Fig. 1B) indicate that 17 weeks after $CD34^+$ HSC IV injection, the engraftment efficiency exhibited a median level of engraftment of 39.8% (± 3.11). No significant difference in engraftment level was observed between the Sham and DMM groups throughout the experimental procedure. Consistent with our flow cytometry data, our immunohistochemical analyses (Fig. 1C) revealed increased immunostaining for human mitochondria and human CD45 in the spleens of the animals exhibiting the highest level of engraftment efficiency, which correlates with the engraftment efficiency assessed in peripheral blood 17 weeks post-humanization. Among the $hCD45^+$ cells, we detected the presence of $hCD3^+$, $hCD19^+$, $hCD14^+$, and $hCD56^+$ cells 17 weeks after the humanization procedure (Fig. 1D) confirming the development of multiple immune cell lineages. The $hCD19^+$ cells that represent the main population in the $hCD45^+$ cell before the surgery exhibit a 1.4-fold and a 2.5-fold decrease in their proportion at 6 and 12 weeks, respectively, post-surgery. By contrast, the proportion of $hCD3^+$-positive cells exhibited a 3-fold and a 6-fold increase at 6 and 12 weeks, respectively, post-surgery. The $hCD14^+$ and the $hCD56^+$ proportions remained relatively stable around 5.5% and 1.5%, respectively, throughout the experiments. The subpopulation repartition in the sham group and the DMM group did not exhibit any statistical differences (data not shown). Human CD19-, CD14-, and CD56-positive cells were also detected in the spleens of the humanized mice (Fig. 1E).

These results clearly indicate that the NSG mice reconstituted with human $CD34^+$ HSCs exhibited engraftment and multilineage development of human immune cells.

Humanized NSG mice developed OA following DMM surgery

Following the surgical induction of OA, the mice recovered quickly and the DMM procedure resulted in the development of cartilage damage over time compared to the sham-operated knees in the humanized mice. Indeed, as evidenced by the Safranin-O staining (Fig. 2A), the articular cartilage in the DMM-operated knees exhibited fibrillation of cartilage surface at 6 weeks and articular cartilage delamination at 12 weeks post-surgery. These cartilage lesions were quantified using a modified OARSI score[19]. A statistically significant increase in the OARSI score was observed from one-week post-surgery to 6 and 12 weeks post-surgery in the DMM group of humanized mice (Fig. 2B). Of note, the OARSI scores were higher in the DMM group than in the sham group at each time point (Fig. 2B). Surprisingly, the non-humanized mice exhibited similar OARSI scores in the Sham and DMM groups at both time points.

The articular cartilage matrix also exhibited structural alteration. Although the type II collagen immunostaining did not show a significant change in the DMM group compared with the sham group 12 weeks post-surgery, a trend towards a decrease in type II collagen staining in cartilage could be discerned over time (Fig. 2C). Type X collagen immunostaining was observed in the cartilage matrix as soon as one week post-surgery. Over time, a change in the localization of the type X collagen immunostaining was observed in the DMM group (Fig. 2C). Indeed, whereas intense staining was observed only in the deep zone 6 weeks post-surgery, this staining extended from the deep zone to the superficial zone at 12 weeks post-surgery (Fig. 2C). We also observed positive staining for the aggrecan cleavage neoepitope NITEGE in the cytoplasm of chondrocytes as early as one week post OA induction (Fig. 2D). At 6 weeks post-surgery, NITEGE staining was observed in the matrix surrounding the chondrocytes. This positive staining of the extracellular matrix for NITEGE was more intense and it surrounded greater numbers of chondrocytes at 12 weeks post-OA induction, whereas the staining remained cytoplasmic in the sham group (Fig. 2D).

Having demonstrated that the DMM surgery induced a significant increase in the OARSI score as well as alteration of the knee cartilage matrix of the humanized mice, we investigated whether the DMM surgery also induced pathological changes in the meniscus of humanized mice, as has been reported in non-humanized wild type mice[23]. We observed that the menisci developed lesions following the DMM procedure (Fig. 3A). Safranin-O fast green histological staining revealed morphological changes in the menisci, with enlargement of the outer part of the menisci near the medial collateral ligament at 6 and 12 weeks post-DMM surgery (Fig. 3A, black arrows) in humanized. An increased degree of ossification was also observed in the menisci 12 weeks after the OA induction (Fig. 3A, white arrows). These lesions were quantified in humanized and non-humanized NSG mice using the scoring system described by Kwok *et al*.[3]. An increase in the meniscal score was observed between one week post-surgery and 12 weeks post-surgery in the DMM group (Fig. 3B). Interestingly, the meniscal score was higher in the DMM group than in the sham group at each time point for humanized mice (Fig. 3B). A similar trend was observed in the non-humanized NSG mice. Regarding the matrix changes in the meniscus, the type II collagen staining was more intense in meniscus one week post-surgery than at the later time points, and it appeared to decrease over time mainly in the mid outer zone of the meniscus (Fig. 3C, black arrows). By contrast, the type X collagen staining increased over time starting, as early as one week in the outer part of the meniscus and reaching the inner part of the meniscus 12 weeks post-DMM (Fig. 3C). Quantified of the meniscal mineralized tissue volume by μCT analysis indicated that 12 weeks post-surgery there was a significant increase in the mineralized tissue volume in the medial meniscus of the DMM group compared to the sham group in humanized mice (Fig. 3D). However, non-humanized mice showed only a trend towards an increased volume of the medial meniscus in the DMM group. All of these results indicated that humanized mice develop OA-associated lesions in the menisci following the DMM procedure.

No significant subchondral bone modification was measured in humanized mice (Supplementary Fig 1 B). Only the cortical bone volume of the DMM group at 12 weeks of the non-humanized mice exhibited a significant increase compared to the sham group. Since equivalent Tunel staining (data not shown) was observed between humanized and non–humanized mice, this difference may not be attributed to increased cell death in humanized mice.

Inflammation and human immune cell infiltration in the joint area of humanized mice

While synovitis has been described as occurring early after the induction of osteoarthritis by DMM[24] in mice, we were interested in determining whether humanized mice also exhibited inflammation of the synovium early after OA induction. Our histological analyses indicate that both the sham group and the DMM group exhibited thickening and an increase in cell density of the synovium (Fig. 4A). Consistent with this, the synovitis scores were higher in the DMM group compared to the sham group at each time point (Fig 4B) in humanized mice. Although the synovitis score decreased over time in both the sham group and the DMM group, it remained higher in the DMM group than in the sham group at 12 weeks post-surgery, thus suggesting continued low-grade inflammation in the synovium of the DMM group (Fig. 4B). In contrast, no significant difference in the synovitis score was evidenced between DMM and sham groups in non-humanized mice

In humanized mice, cells positive for human CD45 (leukocytes) and CD68 (macrophages) were observed in the synovium in the DMM group and the sham group at one week post-surgery (Fig. 4C, black arrows). However, only a few cells were stained 6 and 12 weeks post-surgery (Fig. 4C). Interestingly, cells immuno-positive for human CD45 and CD68 were observed within the bone marrow of the mice in the sham group and the DMM group at each time point (Fig 4D). Consistent with this, a degree of human immune cell infiltration was also

observed within the cruciate ligament or the lateral synovium in some samples (data not shown).

These results demonstrate that human cells are mainly found in the synovium of humanized mice very early after the induction of OA, thus suggesting that human immune cells may mainly participate in the early phase of the inflammatory process following DMM and that they are likely to be less involved in maintaining low-grade inflammation.

DISCUSSION

The objective of the present study was to develop an experimental model of OA in humanized mice. To do so, we relied on the human SCID-repopulating cell (Hu-SRC-SCID), whereby immunodeficient NSG mice are repopulated by injection of $CD34^+$ HSCs[25]. In the present study, after reconstitution of irradiated NSG mice with human $CD34^+$ HSCs, the mice successfully developed a human immune system, as evidenced by the presence of multilineage cells including T and B lymphocytes, NK cells, and monocytes/macrophages. Interestingly, these humanized mice developed OA lesions in the articular cartilage and menisci in 6 to 12 weeks following the DMM procedure. Moreover, synovial inflammation was observed in the first week following the surgery in the DMM group and the sham group, with the presence of human macrophages and human leukocytes. Although this synovitis was greater in the DMM group compared to the sham group, there was a high degree of synovitis in the sham group one week post-surgery due to the sham surgical procedure. Although the synovitis score decreased over time in both the sham group and the DMM group, the synovitis remained more pronounced in the DMM group at each time point, thus suggesting continued low-grade inflammation in the DMM group. Of note, no significant difference in meniscal and synovitis scores was observed in non-humanized mice strengthening the role of the immune system in the development of OA disease.

Among the various mouse models of OA, surgically-induced OA models such as Anterior Cruciate Ligament Transection (ACLT) and DMM[26] are widely acknowledged to satisfactorily, albeit only partially, mimic the onset and progression of the human disease. Since DMM is likely one of the most widely used post-traumatic OA models, we sought to determine whether, in this model, humanized mice develop an OA that is essentially identical to what is observed in non-humanized mice[27]. In conventional non-humanized mice and after an initial inflammatory stage[28], DMM has been reported to induce progressive cartilage degradation, osteophyte formation, modest synovial hypertrophy, and late-onset spontaneous pain[27]. Interestingly, we have demonstrated that our humanized NSG mice developed cartilage and meniscal progressive degradation associated with a significant, albeit only moderate, synovial inflammation, which are similar characteristics to the OA lesions typically observed in the DMM models. Other induced models of OA comprise collagenase-induced OA (CIOA). Although CIOA is less similar to the natural OA progression in humans compared to the DMM model, it is a more inflammatory OA model. It would also be interesting to apply this CIOA model in humanized mice, as this model is often used to investigate pain, inflammation, as well as mesenchymal stem cell therapy in OA[29].

Surprisingly, while we were able to detect cartilage and meniscal alterations in our humanized mice after DMM surgery, we were unable to detect any subchondral bone modifications[30] as generally reported in the DMM OA model whereas non-humanized mice exihibit significant medial subchondral bone plate thickening (Supplementary Fig. 1). One explanation for these unexpected results is that this may be due to the humanization procedure involving 1.5 Gy irradiation before reconstitution of the NSG mice with human $CD34^+$ HSCs. Indeed, such irradiation is known to dramatically disrupt bone marrow and bone metabolism[31,32], which can alter its ability to adapt to the diseased osteoarthritic environment. This observation raises the hypothesis that this model could not be adequate for investigation of subchondral bone

modifications associated with OA progression. This humanized NSG mice model is also restricted in its duration of post-humanization use. Indeed, long-time humanized NSG mice possibly develop graft-versus-host disease, preventing the evaluation of pain associated with osteoarthritis onset which appears around 11-12 weeks after the induction of osteoarthritis in the DMM model[33].

In addition to the Hu-SRC-SCID engraftment procedure used in this study, which allows development of all hematopoietic cell lineages, including T cells, B cells, NK cells, and myeloid cells, various basic approaches to engraft a human immune system have been tested. The Human Blood Lymphocytes SCID (Hu-PBL-SCID), which is the simplest method and consists of injection of human peripheral blood mononuclear cells, allows rapid expansion of human lymphocytes. This Hu-PBL-SCID is limited, however, by only a minor degree of myeloid and B cell development and by the underlying xenogeneic graft-versus-host disease (GVHD) that occurs in 4 to 8 weeks[34], which is too fast compared to the kinetic of OA development. The Bone Marrow-Liver-Thymus (BLT) model, which consists of grafting $CD34^+$ HSCs with human fetal liver and thymus fragments grafted under the renal capsule has also been reported to be a way to generate humanized mice. However, while it is efficient, the generation of BLT mice requires high-level surgical skills, and the availability of human fetal tissues remains limited. Moreover, these BLT mice on the NSG background are highly prone to the development of a wasting GVHD-like disease, which diminishes the usefulness of this model. Given the previously mentioned limitations of the Hu-PBL-SCID and BLT models, the ease of the Hu-SRC-SCID engraftment procedure is likely to represent a user-friendly and scientifically sound compromise.

Although it is a relevant compromise, the humanized mice on the NSG background also exhibit several limitations, in particular, impaired maturation of B and T cells due to the lack of human-specific cytokines and the development of T cells restricted to the mouse major

histocompatibility complex (MHC)[12]. Another hypothetical restriction associated with the NSG strain could be related to its deficiency in complement component 5 (C5). As C5 has been proposed to play a role in the pathogenesis of OA[35], its absence in this model hence has to be carefully considered when planning certain complement-related investigations in this model.

Improved immunodeficient mouse strains for the production of humanized mice have also been generated recently, and they appear to support efficient development of myeloid and lymphoid cells. Of particular interest, MISTRG[36] and QUAD[37] mice have been shown to exhibit development of mature human macrophages and human inflammatory cytokines. Since macrophages are the main immune cells present in the synovial membrane, and a multitude of cytokines are found in the synovial fluid of OA patients, both of these mouse strains could be of interest for further investigation of the role of human macrophages in OA onset and progression. Whether humanized MISTRG, QUAD, or NSG mice will allow assessment of new therapeutic strategies with an improved level of clinical predictivity now warrants further investigation, especially for DMOADs targeting the inflammatory process or to evaluate stem cell-based therapies.

CONCLUSION

Altogether, this study demonstrates for the first time that humanized NSG mice develop post-traumatic OA after surgical induction. Being able to induce OA in humanized mice provides a useful tool to better understand how the human immune system responds during OA, and it may help the development of future therapies with improved efficacies as well as greater selectivity.

ACKNOWLEDGMENTS

The authors would like to thank Martial Masson and MicroPICell Core Facility of Nantes University.

AUTHOR CONTRIBUTIONS

CV and JG conceived the study, designed and supervised the experiments. CV, BB, MAB, BM, CB, CaV, JL, JV, VD, FH performed the experiments. BB, CV, MAB, CB, BM and YM analyzed data and/or provided samples. BB, MAB, CV, JG, and FD wrote the manuscript. CV, JG, and FD provided financial support. All of the authors have read and approved the final manuscript.

FUNDING SOURCE

This work was supported by grants from the French ROAD (Research on OsteoArthritis Diseases) Network, Arthritis R&D, the "Société Française de Rhumatologie", the Agence de la Biomedecine (18GREFFE012), and the Agence Nationale de la Recherche (ANR) through the project PPAROA (ANR-18-CE18-0010-01; JG, CV, FD). BB received a fellowship from "Inserm Region Pays de la Loire". MAB received a fellowship from the FRM (grant ARF202004011786). The humanized rodent platform was supported by the Labex IGO project (n° ANR-11-LABX-0016-01) funded by the Programme d'Investissements d'Avenir, which is a French Government program managed by the French National Research Agency (ANR).

COMPETING INTERESTS

All of the authors declare no conflicts of interest.

REFERENCES

1. Scanzello CR. Role of low-grade inflammation in osteoarthritis. Curr Opin Rheumatol 2017; 29: 79-85;doi.10.1097/BOR.0000000000000353
2. Berenbaum F. Osteoarthritis as an inflammatory disease (osteoarthritis is not osteoarthrosis!). Osteoarthritis Cartilage 2013; 21: 16-21;doi.10.1016/j.joca.2012.11.012
3. Kwok J, Onuma H, Olmer M, Lotz MK, Grogan SP, D'Lima DD. Histopathological analyses of murine menisci: implications for joint aging and osteoarthritis. Osteoarthritis Cartilage 2016; 24: 709-18;doi.10.1016/j.joca.2015.11.006
4. Raghu H, Lepus CM, Wang Q, Wong HH, Lingampalli N, Oliviero F*, et al.* CCL2/CCR2, but not CCL5/CCR5, mediates monocyte recruitment, inflammation and cartilage destruction in osteoarthritis. Ann Rheum Dis 2017; 76: 914-22;doi.10.1136/annrheumdis-2016-210426

5. Oo WM, Hunter DJ. Disease modification in osteoarthritis: are we there yet? Clin Exp Rheumatol 2019; 37 Suppl 120: 135-40;
6. Malfait AM, Little CB. On the predictive utility of animal models of osteoarthritis. Arthritis Res Ther 2015; 17: 225;doi.10.1186/s13075-015-0747-6
7. Seok J, Warren HS, Cuenca AG, Mindrinos MN, Baker HV, Xu W, *et al.* Genomic responses in mouse models poorly mimic human inflammatory diseases. Proc Natl Acad Sci U S A 2013; 110: 3507-12;doi.10.1073/pnas.1222878110
8. Mestas J, Hughes CCW. Of Mice and Not Men: Differences between Mouse and Human Immunology. The Journal of Immunology 2004; 172: 2731-8;doi.10.4049/jimmunol.172.5.2731
9. Schneemann M, Schoeden G. Macrophage biology and immunology: man is not a mouse. Journal of Leukocyte Biology 2007; 81: 579-;doi.10.1189/jlb.1106702
10. Shultz LD, Ishikawa F, Greiner DL. Humanized mice in translational biomedical research. Nat Rev Immunol 2007; 7: 118-30;doi.10.1038/nri2017
11. Foreman O, Kavirayani AM, Griffey SM, Reader R, Shultz LD. Opportunistic bacterial infections in breeding colonies of the NSG mouse strain. Vet Pathol 2011; 48: 495-9;doi.10.1177/0300985810378282
12. Shultz LD, Brehm MA, Garcia-Martinez JV, Greiner DL. Humanized mice for immune system investigation: progress, promise and challenges. Nature Publishing Group 2012; 12: 786-98;doi.10.1038/nri3311
13. Wege AK. Humanized Mouse Models for the Preclinical Assessment of Cancer Immunotherapy. BioDrugs 2018; 32: 245-66;doi.10.1007/s40259-018-0275-4
14. King M, Pearson T, Shultz LD, Leif J, Bottino R, Trucco M, *et al.* A new Hu-PBL model for the study of human islet alloreactivity based on NOD-scid mice bearing a targeted mutation in the IL-2 receptor gamma chain gene. Clin Immunol 2008; 126: 303-14;doi.10.1016/j.clim.2007.11.001
15. Sonntag K, Eckert F, Welker C, Muller H, Muller F, Zips D, *et al.* Chronic graft-versus-host-disease in CD34(+)-humanized NSG mice is associated with human susceptibility HLA haplotypes for autoimmune disease. J Autoimmun 2015; 62: 55-66;doi.10.1016/j.jaut.2015.06.006
16. Misharin AV, Haines GK, 3rd, Rose S, Gierut AK, Hotchkiss RS, Perlman H. Development of a new humanized mouse model to study acute inflammatory arthritis. J Transl Med 2012; 10: 190;doi.10.1186/1479-5876-10-190
17. Glasson SS, Blanchet TJ, Morris EA. The surgical destabilization of the medial meniscus (DMM) model of osteoarthritis in the 129/SvEv mouse. Osteoarthritis and Cartilage 2007; 15: 1061-9;doi.10.1016/j.joca.2007.03.006
18. Bouxsein ML, Boyd SK, Christiansen BA, Guldberg RE, Jepsen KJ, Muller R. Guidelines for assessment of bone microstructure in rodents using micro-computed tomography. J Bone Miner Res 2010; 25: 1468-86;doi.10.1002/jbmr.141
19. Mevel E, Merceron C, Vinatier C, Krisa S, Richard T, Masson M, *et al.* Olive and grape seed extract prevents post-traumatic osteoarthritis damages and exhibits in vitro anti IL-1beta activities before and after oral consumption. Sci Rep 2016; 6: 33527;doi.10.1038/srep33527
20. Glasson SS, Chambers MG, van den Berg WB, Little CB. The OARSI histopathology initiative - recommendations for histological assessments of osteoarthritis in the mouse. Osteoarthritis and cartilage / OARS, Osteoarthritis Research Society; 2010. p. S17-23.
21. Pritzker KP, Gay S, Jimenez SA, Ostergaard K, Pelletier JP, Revell PA, *et al.* Osteoarthritis cartilage histopathology: grading and staging. Osteoarthritis Cartilage 2006; 14: 13-29;doi.10.1016/j.joca.2005.07.014

22. Lewis JS, Hembree WC, Furman BD, Tippets L, Cattel D, Huebner JL*, et al.* Acute joint pathology and synovial inflammation is associated with increased intra-articular fracture severity in the mouse knee. Osteoarthritis Cartilage 2011; 19: 864-73;doi.10.1016/j.joca.2011.04.011
23. Ramos-Mucci L, Javaheri B, van 't Hof R, Bou-Gharios G, Pitsillides AA, Comerford E*, et al.* Meniscal and ligament modifications in spontaneous and post-traumatic mouse models of osteoarthritis. Arthritis Res Ther 2020; 22: 171;doi.10.1186/s13075-020-02261-5
24. Jackson MT, Moradi B, Zaki S, Smith MM, McCracken S, Smith SM*, et al.* Depletion of protease-activated receptor 2 but not protease-activated receptor 1 may confer protection against osteoarthritis in mice through extracartilaginous mechanisms. Arthritis Rheumatol 2014; 66: 3337-48;doi.10.1002/art.38876
25. Shultz LD, Lyons BL, Burzenski LM, Gott B, Chen X, Chaleff S*, et al.* Human Lymphoid and Myeloid Cell Development in NOD/LtSz-scid IL2R null Mice Engrafted with Mobilized Human Hemopoietic Stem Cells. The Journal of Immunology 2005; 174: 6477-89;doi.10.4049/jimmunol.174.10.6477
26. Kuyinu EL, Narayanan G, Nair LS, Laurencin CT. Animal models of osteoarthritis: classification, update, and measurement of outcomes. J Orthop Surg Res 2016; 11: 19;doi.10.1186/s13018-016-0346-5
27. Culley KL, Dragomir CL, Chang J, Wondimu EB, Coico J, Plumb DA*, et al.* Mouse models of osteoarthritis: surgical model of posttraumatic osteoarthritis induced by destabilization of the medial meniscus. Methods Mol Biol 2015; 1226: 143-73;doi.10.1007/978-1-4939-1619-1_12
28. Kung LHW, Ravi V, Rowley L, Bell KM, Little CB, Bateman JF. Comprehensive Expression Analysis of microRNAs and mRNAs in Synovial Tissue from a Mouse Model of Early Post-Traumatic Osteoarthritis. Sci Rep 2017; 7: 17701;doi.10.1038/s41598-017-17545-1
29. Cope PJ, Ourradi K, Li Y, Sharif M. Models of osteoarthritis: the good, the bad and the promising. Osteoarthritis Cartilage 2019; 27: 230-9;doi.10.1016/j.joca.2018.09.016
30. Maerz T, Kurdziel M, Newton MD, Altman P, Anderson K, Matthew HWT*, et al.* Subchondral and epiphyseal bone remodeling following surgical transection and noninvasive rupture of the anterior cruciate ligament as models of post-traumatic osteoarthritis. Osteoarthritis and cartilage / OARS, Osteoarthritis Research Society 2016; 24: 698-708;doi.10.1016/j.joca.2015.11.005
31. Chandra A, Park SS, Pignolo RJ. Potential role of senescence in radiation-induced damage of the aged skeleton. Bone 2019; 120: 423-31;doi.10.1016/j.bone.2018.12.006
32. Costa S, Reagan MR. Therapeutic Irradiation: Consequences for Bone and Bone Marrow Adipose Tissue. Front Endocrinol (Lausanne) 2019; 10: 587;doi.10.3389/fendo.2019.00587
33. Driscoll C, Chanalaris A, Knights C, Ismail H, Sacitharan PK, Gentry C*, et al.* Nociceptive Sensitizers Are Regulated in Damaged Joint Tissues, Including Articular Cartilage, When Osteoarthritic Mice Display Pain Behavior. Arthritis Rheumatol 2016; 68: 857-67;doi.10.1002/art.39523
34. Ito R, Katano I, Kawai K, Hirata H, Ogura T, Kamisako T*, et al.* Highly sensitive model for xenogenic GVHD using severe immunodeficient NOG mice. Transplantation 2009; 87: 1654-8;doi.10.1097/TP.0b013e3181a5cb07
35. Wang Q, Rozelle AL, Lepus CM, Scanzello CR, Song JJ, Larsen DM*, et al.* Identification of a central role for complement in osteoarthritis. Nat Med 2011; 17: 1674-9;doi.10.1038/nm.2543

36. Rongvaux A, Willinger T, Martinek J, Strowig T, Gearty SV, Teichmann LL*, et al.* Development and function of human innate immune cells in a humanized mouse model. Nat Biotechnol 2014; 32: 364-72;doi.10.1038/nbt.2858
37. Shultz LD, Keck J, Burzenski L, Jangalwe S, Vaidya S, Greiner DL*, et al.* Humanized mouse models of immunological diseases and precision medicine. Mamm Genome 2019; 30: 123-42;doi.10.1007/s00335-019-09796-2

FIGURE LEGENDS

Figure 1: Validation of the mouse humanization. A) Study workflow. Humanized mice were generated by repopulating irradiated 5-week-old NSG mice with human $CD34^+$ HSCs (Hu-SRC-SCID model). The mice underwent a DMM or a sham procedure 17 weeks post-humanization. The mice were then sacrificed 1, 6, or 12 weeks post-surgery, and samples were prepared for subsequent analyses. **B)** Engraftment efficiency (% Graft) between the different groups. % Graft was calculated as the proportion of human $CD45^+$ cells in the total $CD45^+$ cell population (human and mouse) in peripheral blood. Flow cytometry gating strategy: cells positives for human and mouse CD45 were discriminated. **C)** Immunohistochemical staining for human mitochondria and human CD45 in the spleens of the 12-week-old humanized mice. The scale bar = 100 µm. **D)** Human immune system multilineage development: FACS analysis for human CD3 (T cells), CD19 (B cells), CD14 (monocyte), and CD56 (NK cells) in the human $CD45^+$ cell fraction in the peripheral blood of the humanized mice 17 weeks post-humanization, and 6 and 12 weeks post-DMM or sham surgery. **E)** Immunohistochemical staining for human CD19 (B cells), CD14 (monocyte), and CD56 (NK cells) in the spleens of mice 12 weeks post-DMM or sham surgery. Scale bar = 100 µm. #### $p < 0.0001$, ## $p < 0.01$ (Kruskal-Wallis followed by Dunn's multiple comparisons test) compared to 17 weeks post-humanization.

Figure 2: Articular cartilage changes after DMM in humanized mice. A) Representative Safranin-O fast green-stained sections of articular cartilage from humanized mice 1, 6, and 12 weeks post-surgery. The scale bar = 100 µm. **B)** Modified OARSI score (maximum score = 25) of non-humanized (black line) and humanized mice (red line). ** $p < 0.01$, * $p < 0.05$ (Mann-Whitney), and # $p < 0.05$ (Kruskal-Wallis followed by Dunn's multiple comparisons test). **C)** Representative immunohistochemical staining for type II collagen (COL II) and type X collagen (COLX) of humanized mice knee joints. The scale bar = 100 µm. **D)** Representative

immunohistochemical staining for NITEGE (aggrecan cleavage neoepitope) of humanized mice knee joints. The scale bar = 100 µm. NITEGE enlarged picture, scale bar = 25µm.

Figure 3: Meniscal pathological changes after DMM in humanized mice. A) Representative Safranin-O fast green-stained sections of the medial meniscus from humanized mice 1, 6, and 12 weeks post-surgery. The scale bar = 250 µm. **B)** Meniscal score (maximum score = 15) of non-humanized (black line) and humanized mice (red line). **C)** Representative immunohistochemical staining for type II collagen (COL II) and type X collagen (COLX) in the meniscal matrix of humanized mice OA joints. Scale bar = 250 µm. **D)** Meniscal calcification changes throughout the establishment of the OA. Representative 3D reconstitution and coronal section of humanized mice knee joint illustrating meniscus calcification 6 and 12 weeks post-surgery. Bone Volume (BV) quantification of the medial meniscus of non-humanized (black line) and humanized mice (red line). ** $p < 0.001$, * $p < 0.05$ (Mann-Whitney).

Figure 4: Synovial inflammation following the DMM procedure. A) Representative Safranin-O fast green-stained sections of the synovial membranes of humanized mice 1, 6, and 12 weeks post-DMM or sham surgery. Scale bar = 100 µm. **B**) Synovitis score (maximum score = 6) non-humanized (black line) and humanized (red line) mice. ** $p < 0.001$, * $p < 0.05$ (Mann-Whitney) and ### $p < 0.001$, ## $p < 0.01$ (Kruskal-Wallis followed by Dunn's multiple comparisons). **(C, D)** Human immune cells in the joint area**.** Immunohistochemical staining for human CD45 and CD68 in (C) in the synovial membrane of the humanized mice 1, 6, and 12 weeks post-DMM surgery. Black arrows indicate positive cells, the scale bar = 100µm. (D) the bone marrow of the humanized mice 1, 6, and 12 weeks post-DMM surgery. Scale bar = 100 µm.

Supplementary Figure 1: Microtomography assessment of subchondral bone changes after DMM in humanized mice. A) Representative 3D reconstitution of the tibia and selection

of the region of interest (ROI) for analysis. Following the spatial orientation and the selection of a cylindrical ROI in the medial side of the tibia (upper left panel: posterior view of the tibia; upper right panel: top view of the medial tibial plateau and the ROI in blue), the ROI was divided into a cortical and a trabecular area (lower panel). **B)** Quantification of the bone volume (BV) of the total ROI, cortical and trabecular areas (upper panel and lower left panel) and the trabecular thickness (Tb.Th) of the trabecular area (lower right panel) in non-humanized control (black bars) and humanized mice (red bars) sham (empty bars) or DMM (plain grey bars). * $p < 0.05$ (Kruskal-Wallis followed by Dunn's multiple comparisons test).

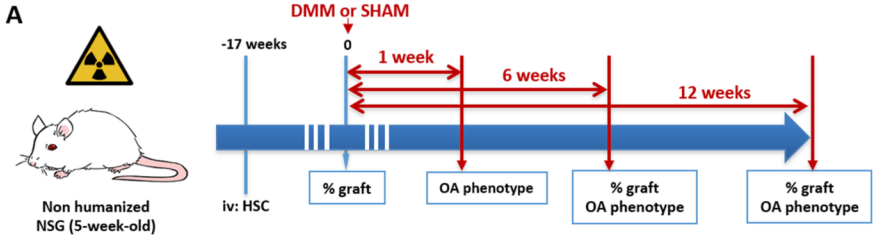
A
DMM or SHAM
-17 weeks
0
1 week
6 weeks
12 weeks
Non humanized
NSG (5-week-old)
iv: HSC
% graft
OA phenotype
% graft
OA phenotype
% graft
OA phenotype

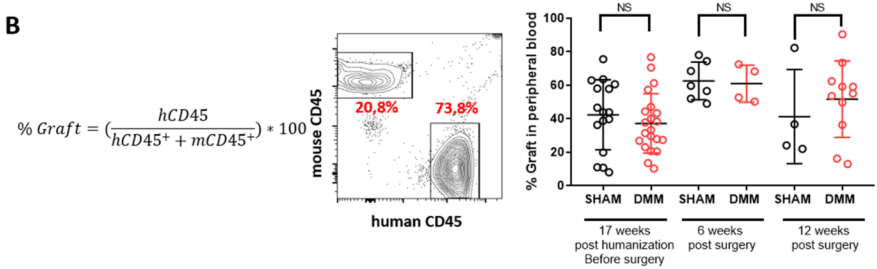
B
$\% Graft = (\frac{hCD45}{hCD45^{+} + mCD45^{+}}) * 100$
20,8%
73,8%
mouse CD45
human CD45
% Graft in peripheral blood
NS
NS
NS
SHAM
DMM
SHAM
DMM
SHAM
DMM
17 weeks
post humanization
Before surgery
6 weeks
post surgery
12 weeks
post surgery

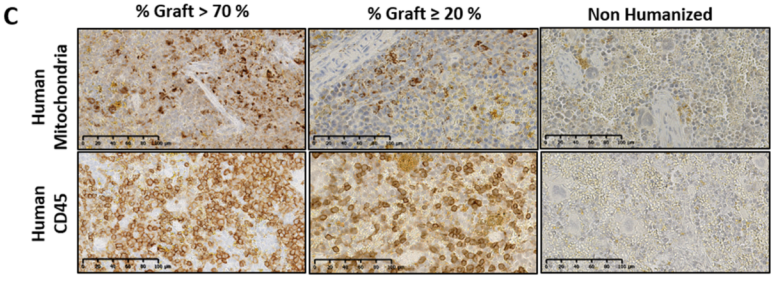
C
% Graft > 70 %
% Graft ≥ 20 %
Non Humanized
Human Mitochondria
Human CD45

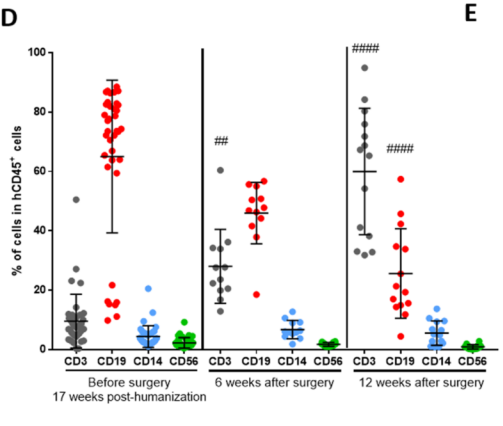
D
% of cells in hCD45+ cells
CD3
CD19
CD14
CD56
Before surgery
17 weeks post-humanization
6 weeks after surgery
12 weeks after surgery
##
####
####

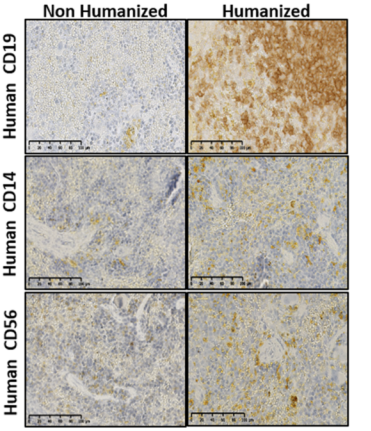
E
Non Humanized
Humanized
Human CD19
Human CD14
Human CD56

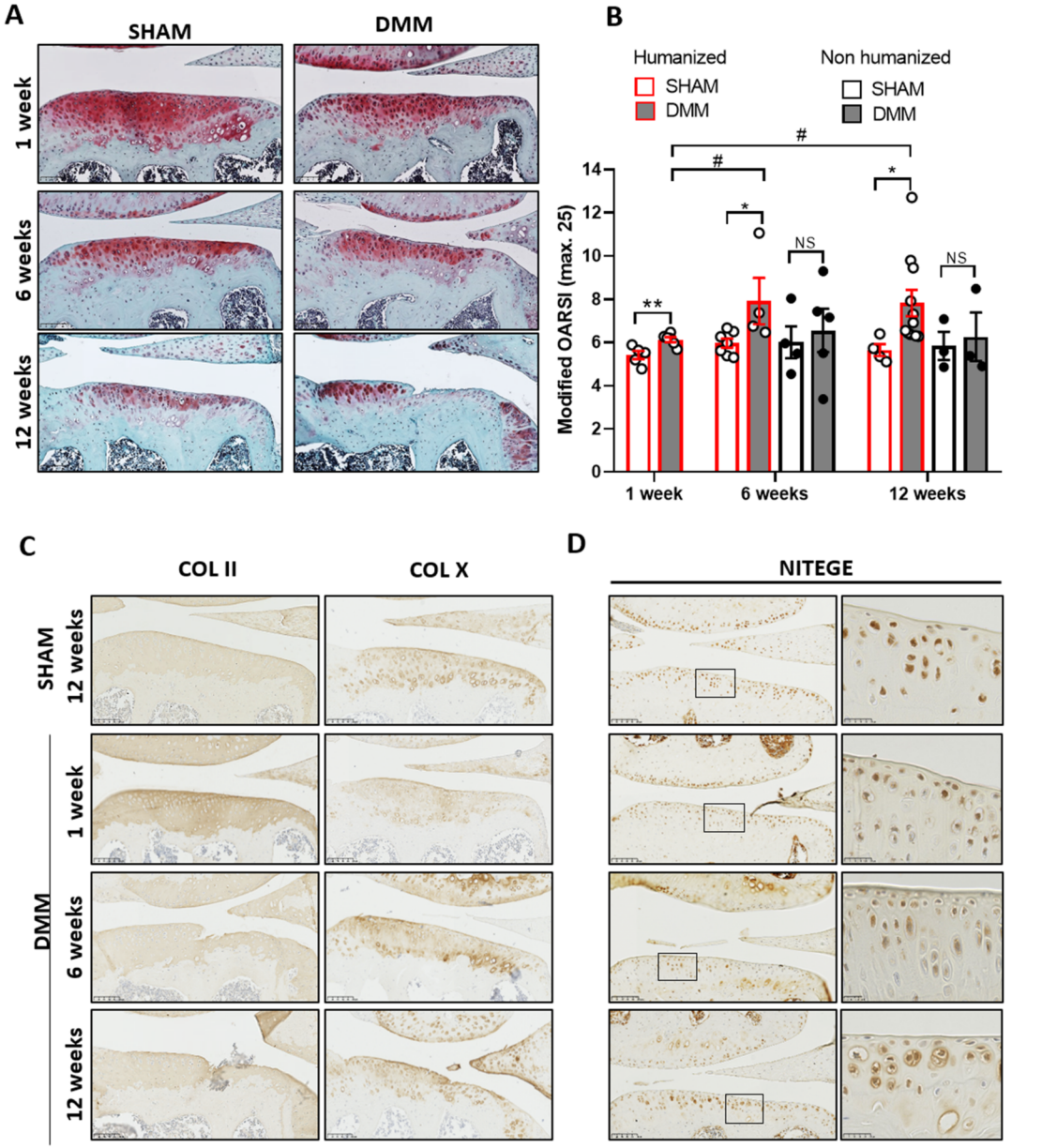
A
SHAM
DMM
1 week
6 weeks
12 weeks
B
Humanized
SHAM
DMM
Non humanized
SHAM
DMM
Modified OARSI (max. 25)
0
2
4
6
8
10
12
14
#
#
*
*
NS
NS
**
1 week
6 weeks
12 weeks
C
COL II
COL X
SHAM
12 weeks
DMM
1 week
6 weeks
12 weeks
D
NITEGE

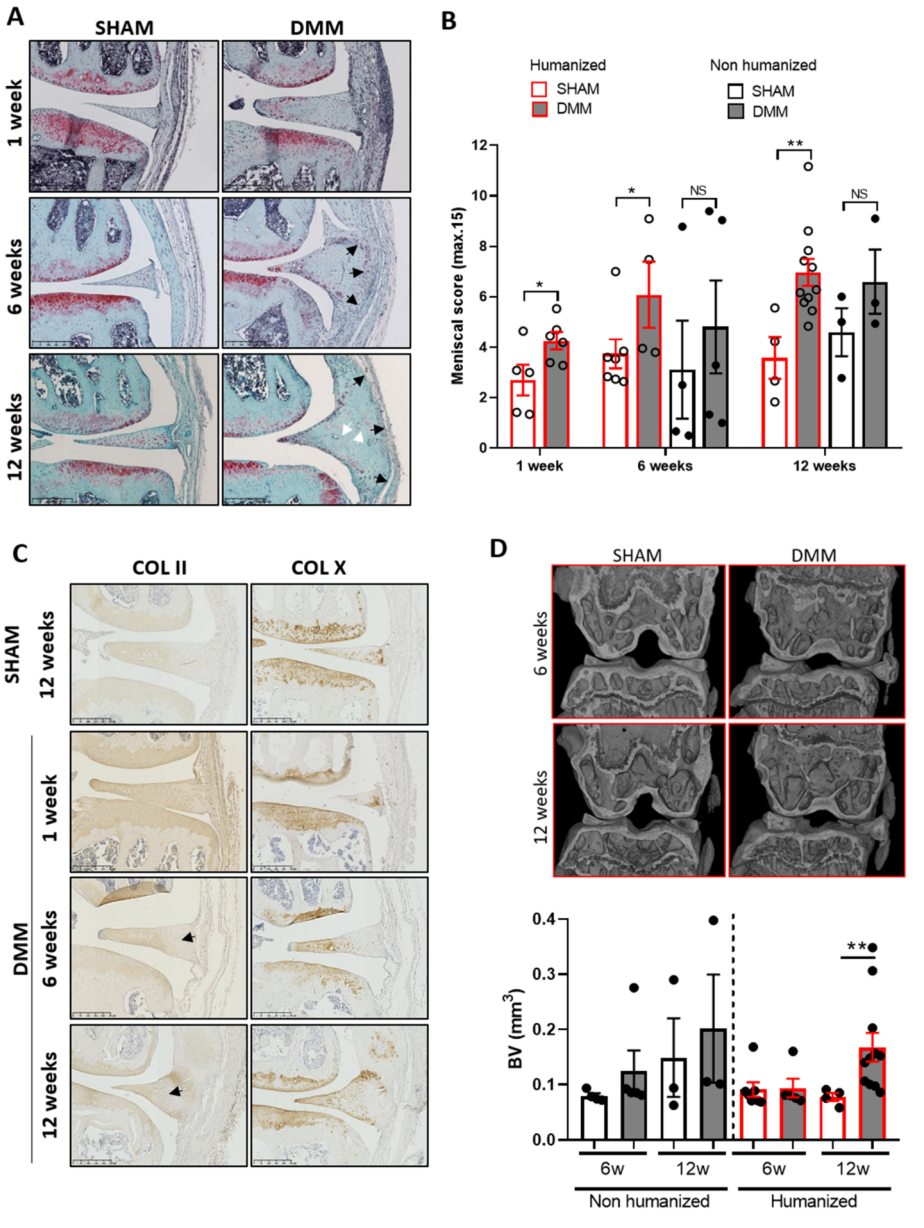
A
SHAM
DMM
1 week
6 weeks
12 weeks
B
Humanized
SHAM
DMM
Non humanized
SHAM
DMM
Meniscal score (max.15)
12
10
8
6
4
2
0
*
*
NS
**
NS
1 week
6 weeks
12 weeks
C
COL II
COL X
SHAM
12 weeks
DMM
1 week
6 weeks
12 weeks
D
SHAM
DMM
6 weeks
12 weeks
BV (mm3)
0.4
0.3
0.2
0.1
0.0
**
6w
12w
6w
12w
Non humanized
Humanized

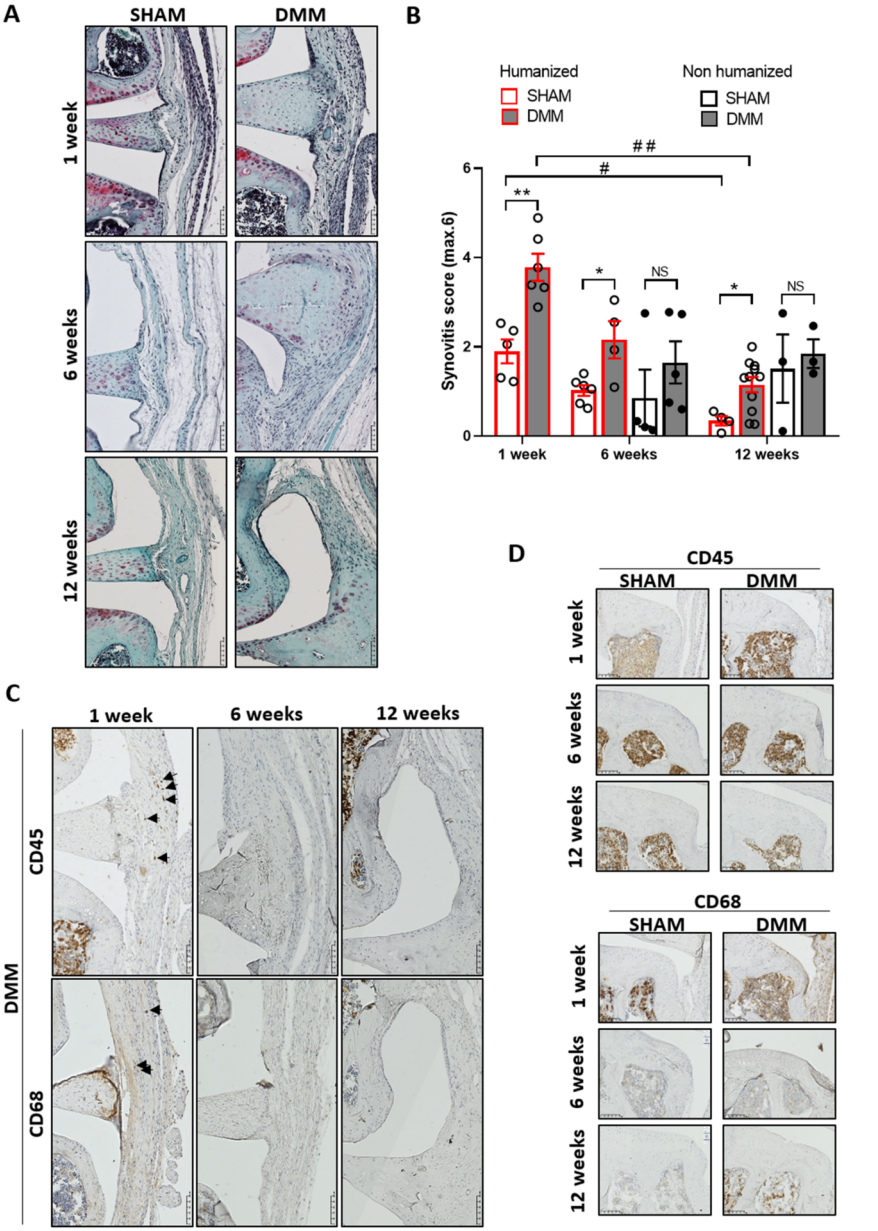
A
SHAM
DMM
1 week
6 weeks
12 weeks
B
Humanized
SHAM
DMM
Non humanized
SHAM
DMM
Synovitis score (max.6)
**
#
##
*
NS
*
NS
1 week
6 weeks
12 weeks
C
1 week
6 weeks
12 weeks
DMM
CD45
CD68
D
CD45
SHAM
DMM
1 week
6 weeks
12 weeks
CD68
SHAM
DMM
1 week
6 weeks
12 weeks

Table 1: List of antibody used for flow cytometry and immunohistochemistry (IHC)

	Target	Ref	Provider
Flow cytometry	mouse CD45- PerCp Cy5.5	30F11	BD Biosciences, USA
	human CD45-PE Cy7	HI30	
	human CD3-PE	UCHT1	
	human CD19-FITC	HIB19	
	human CD14-Pacific Blue™	M5E2	
	human CD56-Alexa Fluor® 647	B159	
IHC	mouse Type II collagen	ab34712	Abcam, UK
	mouse type X collagen	1-CO097-05	Quartett Immunodiagnostics, Germany
	mouse NITEGE	PA1-1746	
	human mitochondria	K8000	Agilent, CA, USA
	human CD45	M0701	
	human CD19	M7296	
	human CD14	M7304	
	human CD56	M0825	
	human CD68	M0876	

Table 2: The cartilage scoring system used to evaluate OA severity (adapted from Glasson S.S., *et al*., 2010 and Pritzker K.P., *et al*., 2005).

Scoring category	Observation	Score
Chondrocyte death	None	0
	≤ 10%	1
	≤ 25%	2
	≤ 50%	3
	≤ 75%	4
	≤ 100%	5
Chondrocyte hypertrophy	None	0
	Presence	1
Chondrocyte clusters	None	0
	Superficial zone	1
	Middle zone	2
	Complex structure	3
	Cyst formation	4
Loss of Safranin-O staining	None	0
	Superficial zone of non-calcified cartilage	1
	Middle zone of non-calcified cartilage	2
	Non-calcified cartilage and intense staining around clusters	3
	Absent with staining around clusters	4
	Absent	5
Cartilage surface	Intact	0
	Superficial fibrillation or abrasion	1
	Deep fibrillation	2
	Vertical fissures	3
	Delamination / Excavation	4
Bone	None	0
	Denudation	4
	Microfracture	5
	Remodeling	6
	Total	**25**